

# A Retrodirective Array Using Slope Detection and Phase Shifting

#Wade G. Tonaki, Reece T. Iwami, Alexis Zamora, Tyler F. Chun, Wayne A. Shiroma  
Department of Electrical Engineering, University of Hawai'i  
2540 Dole St., Holmes 483, Honolulu, HI, 96822, USA, wtonaki@hawaii.edu

## Abstract

A full-duplex retrodirective array using phase detecting and phase shifting is presented. The system autonomously steers its beam in the direction of an interrogator signal, even after the interrogator is turned off. Retrodirectivity is reported for angles of  $-10^\circ$ ,  $0^\circ$ , and  $+30^\circ$ .

**Keywords :** Phased arrays, Retrodirective arrays

## 1. Introduction

A retrodirective array (RDA) is a class of antenna that autonomously responds to an interrogator without knowing the source of interrogation. This type of antenna is applicable to automatic pointing and tracking systems, radar transponders, self-tracking wireless communication links, and security-sensitive transmissions [1].

Most RDAs demonstrated to date are based on analog circuitry with no digital signal processing [2]-[4]. The analog nature of these RDAs is appealing because of their resulting simplicity compared to smart antennas. However, because these kinds of arrays must process the interrogator signal in some fashion to create the retrodirected signal, it causes them to suffer from the limitation of only being able to retrodirect while being interrogated.

This paper presents a new all-analog RDA architecture that does not suffer from this limitation. That is, it is able to respond to an interrogating source that does not have to be constantly transmitting. As such, it can respond to pulsed interrogating signals such as those in radar.

The operating concept is as follows. Assume that the RDA is interrogated from some unknown direction. To determine the interrogator's direction of arrival (DOA), the RDA scans the entire visible half-plane while detecting the direction of maximum received power (and thus the DOA). Next, analog control circuitry sets up the phasing that results in a retrodirected beam back in the interrogating direction.

## 2. Design

Fig. 1 illustrates the proposed system, which is composed of a phase detector, phase-shifting module, and control circuit. The phase detector, consisting of a maximum-power detecting circuit, determines the DOA. A control circuit then outputs the necessary phase-shifter control voltages that results in a retrodirected beam back in the interrogating direction.

### 2.1 Beam Scanning

Determination of the DOA begins by scanning the entire visible half-plane for RF power. This technique was previously demonstrated in [5], but had to operate in power-detection and retrodirection modes sequentially, rather than simultaneously. It was also only capable of half-duplex communication.

In contrast, the architecture proposed in this paper is capable of simultaneously scanning and communicating in full-duplex mode. The DOA determination scheme uses only the two center elements of the array in Fig. 1(a), shown in more detail in Fig. 2. The entire visible half-plane is scanned from  $-90^\circ \leq \theta \leq +90^\circ$  for RF power at the 8.1-GHz interrogating frequency, where  $\theta$  is the scan angle from broadside. Scanning is performed by adjusting  $V_{scan}$ , which controls phase shifter PS1, while maintaining  $V_{fix} = 0$  V, which fixes phase shifter PS2 to some reference phase. The result

is  $\Phi$ , the phase difference between the two center elements in reference to PS2. PS1 and PS2 are implemented with Hittite HMC538 phase shifters.

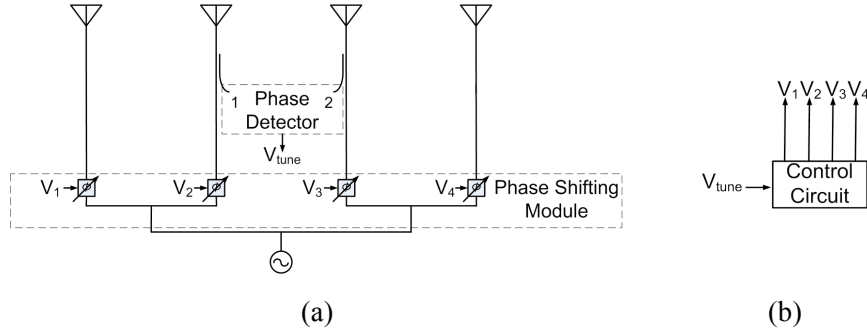


Fig. 1: Schematic of four-element retrodirective array using a phase detector and phase shifting, showing the three major modules: (a) phase-detector and phase-shifting module, and (b) control circuit.

$V_{scan}$  for PS1 is adjusted via an 8-bit digital counter that iterates through its 256 values and feeds an Analog Devices AD7224 DAC. This provides a  $0.7^\circ$  resolution in  $\theta$  for a single counter iteration. The DAC outputs a ramp voltage between 0-1.82 V that corresponds to the  $0^\circ$ - $360^\circ$  phase shift  $\Phi$  applied by PS1.

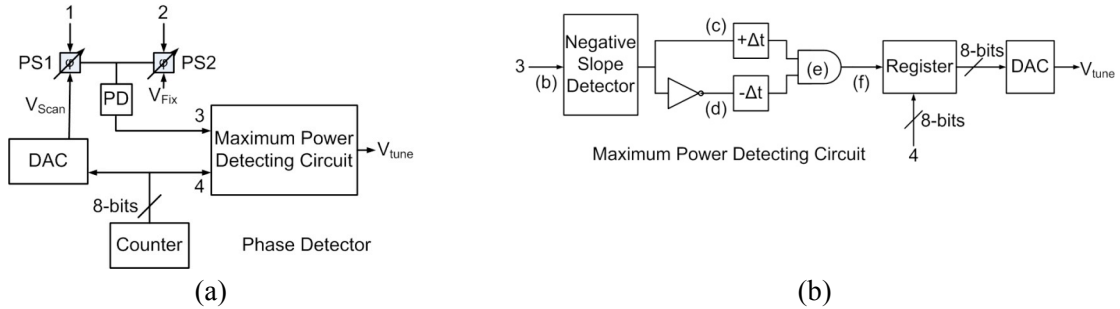


Fig. 2: (a) DOA determination scheme where Ports 1 and 2 correspond to those in Fig. 1(a); (b) Schematic of maximum-power detecting circuit where Ports 3 and 4 correspond to those in Fig. 2(a) and points (b)-(f) correspond to graphs in Fig. 3.

## 2.2 Phase Detection

As the beam formed by the two center array elements scans the visible half-plane, received power at each of those two elements combine through a 2:1 Wilkinson power combiner, and then feed a power detector, which outputs an analog voltage corresponding to the detected RF. The Hittite HMC611 power detector has an inverse relationship between detected power and output voltage. That is, it outputs a DC voltage minimum when detecting maximum RF power over a sweep, and vice versa.

This voltage is fed to the maximum-power detecting circuit shown in more detail in Fig. 2(b), which also receives input from the counter. The maximum-power detecting circuit outputs a voltage  $V_{tune}$ , proportional to the phase difference between the two antenna elements (and thus, the DOA). This voltage is used by the control circuit, described later in Sec. 2.3, to retrodirect a beam.

Fig. 3 assists in visualizing the DOA determination scheme. Fig. 3(a) shows the DAC ramp signal described earlier in Sec. 2.1. Figs. 3(b)-(f) show the voltages at various points in the schematic of Fig. 2(b), assuming an interrogator located at  $\theta = 0^\circ$ . At point (b), the power-detecting voltage signal is fed to a negative slope detecting circuit, which outputs an analog voltage value of 5 V when the slope is negative and 0 V when it is positive. The negative slope signal is split into two paths, with one path being digitally inverted; these correspond to points (c) and (d). The two signals are then time-shifted in opposite directions, with one being lagged and the other being led and sent to an AND gate that combines the signals at point (e). The output of the AND at point (f) yields a signal that displays locations where maximum power (and thus the interrogator's DOA) is detected.

Upon finding the maximum power, a Motorola MC74F161A 8-bit register simultaneously loads the corresponding 8-bit counter value that was fed to PS1 to another DAC that outputs a tun-

ing voltage,  $V_{tune}$ . This voltage represents the progressive phase shift  $\Phi_p$  needed for the phase-shifting module to retrodirect a signal back in the interrogating direction. When not at a maximum power level, the register holds the last known maximum power digital value as  $V_{tune}$ . Fig. 1(b) shows that  $V_{tune}$  is fed to a control circuit, which then outputs four voltages  $V_1$ - $V_4$  that control the phase shifters that steers a retrodirected signal back to the interrogator.

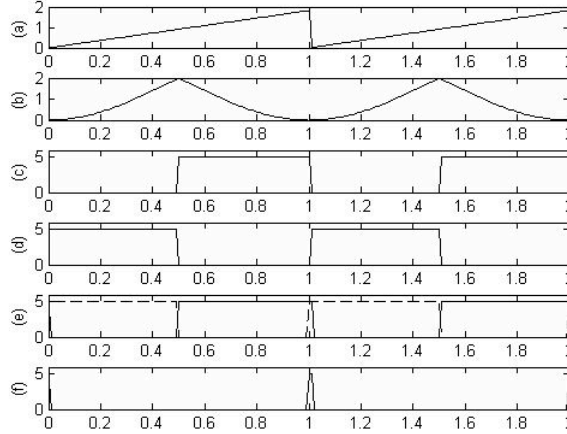


Fig. 3: Voltages at various points of the maximum-power detecting circuit of Fig. 2(b), assuming an interrogator located at  $\theta = 0^\circ$ . X-axis units are in periods. Y-axis units are in volts. (a) ramp voltage controlling PS1 representing a  $0^\circ$ - $360^\circ$  phase shift  $\Phi$ ; (b) power detector voltage; (c)-(e) signals manipulated from (b); (f) maximum power detection.

### 2.3 Phase-Shifting Module

Fig. 1(a) shows the phase-shifting module, where an LO at 8.19 GHz feeds a 1:4 Wilkinson power divider that feeds four parallel HMC538 phase shifters, then four quasi-Yagi antenna elements. The phase-shifting module uses

$$\Phi_p = \frac{2\pi}{\lambda} d \sin \theta, \quad (1)$$

where  $\Phi_p$  is the progressive phase difference between the antenna elements,  $d$  is the antenna element spacing, and  $\lambda$  is the interrogating wavelength.

The phase detector and phase-shifting module are integrated to eliminate the need for separate transmit and receive circuitry. They share a 4-element quasi-Yagi array with a 6.0 – 8.7 GHz bandwidth (37% fractional bandwidth). The transmit and receive frequencies are 8.19 and 8.10 GHz, respectively. The array is fabricated on Rogers TMM10i (thickness = 1.016 mm,  $\epsilon_r = 9.8$ ) and features half-wavelength spacing at 7.82 GHz.

## 3. Experiment

### 3.1 Tracking Capability

Fig. 4(a) shows the monostatic transmit and receive radar cross section (RCS) pattern of the RDA. The plots demonstrate the RDA's active tracking capabilities across its visible range. The transmit setup involved two horns collocated on a sweeping arm that was swept from  $-40^\circ \leq \theta \leq 40^\circ$ . One horn interrogated the RDA at 8.10 GHz, while the other horn received the transmitted response of the RDA at 8.19 GHz. The receive setup used a transmitting horn swept across  $-40^\circ \leq \theta \leq 40^\circ$  while power received at the RDA was recorded. The -10 dB dips between  $-30^\circ$  and  $-20^\circ$  are due to the introduction of additional peaks in Fig. 3(f) that affected the steering of the RDA.

### 3.2 Full-Duplex Operation

Full-duplex operation of the RDA was demonstrated by taking bistatic patterns in both receive and transmit modes. Transmit RCS patterns involved using a static 8.1 GHz interrogating horn, and a second horn, mounted on a rotating arm that is swept from  $-60^\circ \leq \theta \leq 60^\circ$ , measuring the received power from the RDA transmitting at 8.19 GHz. For the receive RCS patterns, an interrogating horn at 8.1 GHz was fixed and the DOA was determined by the RDA. The register was forced into a hold state, keeping the RDA pointing in the same direction, while an 8.19 GHz trans-

mitting horn was swept from  $-60^\circ \leq \theta \leq 60^\circ$ . Power received at the RDA was recorded. Experimental transmit and receive RCS patterns are reported in Fig. 4 for interrogating locations of  $-10^\circ$ ,  $0^\circ$ , and  $30^\circ$ . There is good agreement with the theoretical plots and the experimental plots that highlight the RDA's accurate retrodirective abilities.

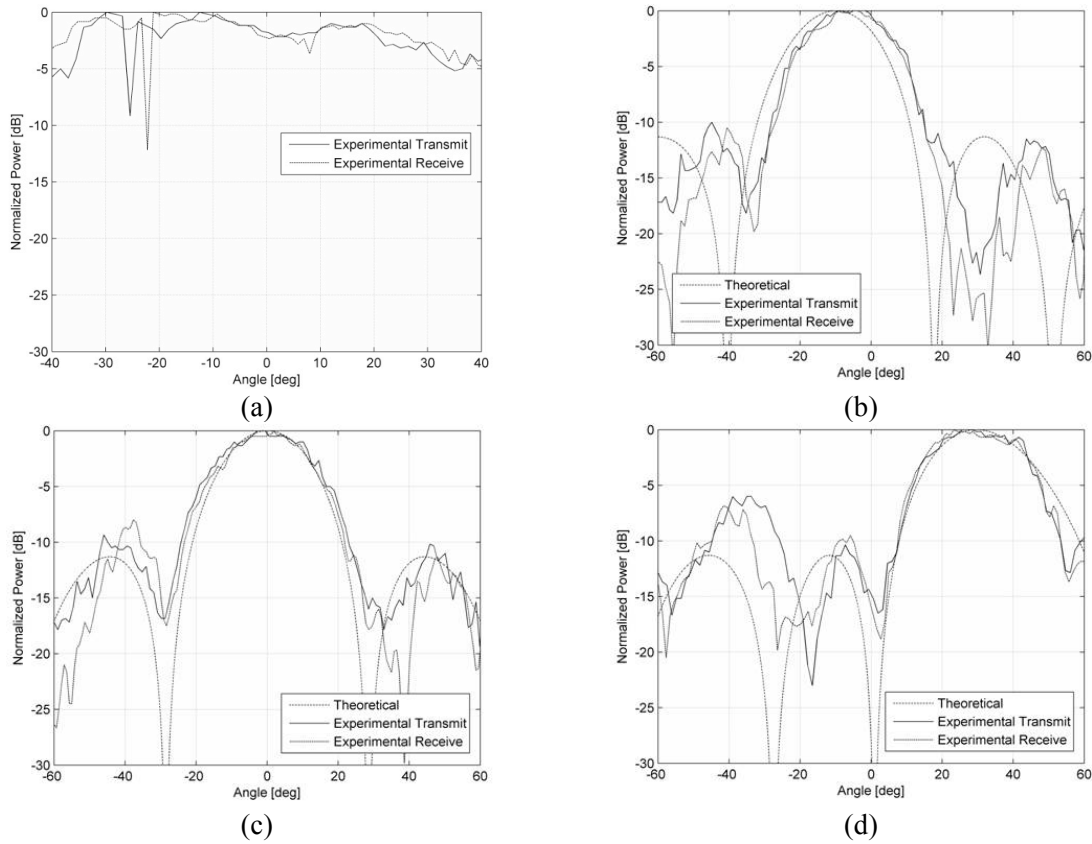


Fig. 4: (a) Monostatic radar cross section for transmit and receive modes; Bistatic radar cross sections with interrogator at: (b)  $-10^\circ$ , (c)  $0^\circ$ , and (d)  $+30^\circ$ . Proper transmit and receive frequency operation demonstrates full-duplex capability.

## 4. Conclusion

A full-duplex, self-steering array has been presented. Phase detection through power detection and slope analysis, along with simplified control circuitry accurately determined the DOA with and without the presence of interrogating signals. The four-element array operated at a receive frequency of 8.10 GHz and transmit frequency of 8.19 GHz. Retrodirectivity was demonstrated for angles of  $-10^\circ$ ,  $0^\circ$ , and  $+30^\circ$ .

## References

- [1] R. Y. Miyamoto and T. Itoh, "Retrodirective arrays for wireless communications," *IEEE Microw. Mag.*, vol. 3, no. 1, pp. 71-79, Mar. 2002.
- [2] C. Y. Pon, "Retrodirective array using the heterodyne technique," *IEEE Trans. Antenna Propag.*, vol. AP-12, pp. 176-180, Dec. 1964.
- [3] G. S. Shiroma, R. Y. Miyamoto, and W. A. Shiroma, "A full-duplex dual-frequency self-steering array using phase detection and phase shifting," *IEEE Trans. Microw. Theory Tech.*, vol. 54, no. 1, pp. 128-134, Jan. 2006.
- [4] T. Brabetz, V. F. Fusco, and S. Karode, "Balanced subharmonic mixers for retrodirective-array applications," *IEEE Trans. Microw. Theory Tech.*, vol. 49, no. 3, pp. 465-469, Mar. 2001.
- [5] J. M. Akagi, A. Zamora, M. K. Watanabe, and W. A. Shiroma, "A self-steering array using power detection and phase shifting," in *IEEE MTT-S Int. Microw. Symp. Dig.*, Atlanta, GA, pp. 1325-1328, Jun. 2008.